Studies on New Delhi Metallo-Beta-Lactamse-1 producing *Acinetobacter baumannii* isolated from donor swab in a tertiary eye care centre, India and structural analysis of its antibiotic binding interactions

Murali Sowmiya[1], Vetrivel Umashankar[2], Sivashanmugan Muthukumaran[2], Hajib Naraharirao Madhavan [1] & Jambulingam Malathi[1]*

[1]L& T Microbiology Research Centre, Vision Research Foundation, Sankara Nethralaya, New.41 (Old.No18), Chennai – 600006 India; [2]Centre of Bioinformatics, Vision Research Foundation, Sankara Nethralaya, Chennai, India; Jambulingam Malathi - Email: drjm@snmail.org; Phone:-+91 44 28220709; Fax : +91 44 28254180; *Corresponding author

Abstract:
Gram-negative bacilli, *Enterobacteriaceae* and *Non-fermentors* with resistance to carbapenems and metallo beta-lactams are the major cause of concern in clinical problems in current human healthcare. The most highly emerging dreadful Metallo Beta-lactamses is New Delhi metallo-beta-lactamase (*bla*NDM-1) which confers resistance to carbapenems; susceptible only to colistin and, less consistently to tigecycline, leading to no therapeutic options. In the present study, we demonstrate the effects of cephalosporins and carbepenems on biofilm producing *A. baumanii* clinical isolate and also to infer the probable inhibitory binding mode through molecular docking studies. The result of MIC on Biofilm producing *A. baumanii* and the docking analysis results were found to be concordant. Moreover, we also found cephalosporins and carbepenem groups to interact with 162-166 region of *bla*NDM-1, which is unique for NDM-1 and also documented to be a potential drug targeting region.

Background:
Antibiotic-resistant Gram-negative bacilli belonging to *Enterobacteriaceae* and *Non-fermentors* are the major cause of concern in clinical problems in current human healthcare [1, 2] Beta-lactams have been the mainstay of treatment for serious infections in humans [3]. Among Gram-negative bacteria, the most common beta-lactam resistance mechanism involves beta-lactamase mediated hydrolysis which results in inactivation of antibiotics which are used in the treatment of infection caused by these organisms and are being reported in increasing frequencies [4]. One of the last lines of treatment against high level drug resistant infections is the carbapenems and are metallo-beta-lactams (MBL) class of antibiotics, which was developed to resist the beta-lactamase mediated resistance posed by infection causing microbes [5, 6]. Recent studies has proved the inactivation of these carbapenams (meropenem, imipenem, doripenem, ertapenem) by a number of metallo-beta-lactamases which poses extended spectrum activity against all beta-lactam antibiotics, including carbapenems [5-7]. One such highly emerging dreadful MBL's is New Delhi metallo-beta-lactamase (*bla*NDM-1). This *bla*NDM-1 is a novel MBL's conferring resistance to almost all beta-lactam antibiotics, including carbapenem [8-11]. Many reports are emerging on the existence and prevalence of *bla*NDM-1 throughout the world [3, 4, 7, & 12]. Microorganisms carrying *bla*NDM-1gene are *E. coli, K. pneumoniae, K. oxytoca, Enterobacter cloacae, Proteus spp., Citrobacter freundii, Morganella morganii, Providencia spp. Pseudomonas aeroginosa* [2, 3, 8] and also in *Acinetobacter*

baumannii [12, 13]. Presence of *bla*NDM-1 gene was also detected among bacteria isolated from seepage samples and public tap waters in New Delhi, India [14]. Many reports have revealed the spread of *bla*NDM-1 through renal or bone marrow transplantation, dialysis, cerebral infarction, chronic obstructive pulmonary disease, pregnancy, burns, road traffic accidents, and cosmetic surgery [3] Hence, the microorganism carrying the *bla*NDM-1 gene will be extensively resistant to antibiotics and susceptible only to colistin and, less consistently, tigecycline, leading to scarcity of antibiotics for treatment [8, 11]. *Acinetobacter baumannii* is a common nosocomial pathogen reported worldwide [15]. Infections caused by *A. baumannii* are associated with adverse clinical outcomes, including high rates of morbidity and mortality, prolonged hospital stay, and substantial health care expenses. Many reports on emergence of *bla*NDM-1 among *A. baumannii* have been reported [13, 16]. In our previous study, we have isolated *blaNDM -1* carrying *A. baumannii* with high drug resistance was isolated from a multiorgan donor. [17]. Though reports on the three dimensional structures of *bla*NDM-1, active site regions, molecular docking and ligands complex molecular dynamic simulation studies in different microbial pathogenic organisms synthesis different protein length of *bla*NDM-1 exist, in this study we aimed to correlate the microbiological investigations carried out to screen its level of drug resistance with that of *in silico* studies of drug interactions using bioinformatics tools.

Methodology:
A. baumanii, isolated from a conjunctival swab collected from a 23 years old multi organ donor, died in a road traffic accident was utilized for this study, after validation through documented bacteriological methods [18]. Further, the isolate was screened for the presence of *bla*NDM-1 at clinical microbiology laboratory of L & T Microbiology Research Centre from Sankara Nethralaya, Chennai. The bacterium was found to harbor the *bla*NDM-1 by PCR based DNA technique and was further sequenced for confirmation. The sequence obtained was submitted to Genbank [Accession no: JF836807].

Biofilm production detection:
Detection of Biofilm production by Tissue culture plate method
Biofilm production of *A. baumanii* isolate was carried out aerobically in 96 well round bottom tissue culture plate as described earlier [19, 20] with slight modifications. The adherent biofilm producing cells was released by adding 160 ml 33% acetic acid (SRL, India). The sterile uninoculated brain heart infusion broth media served as medium control to check sterility. Carbapenem susceptible *K. pneumoniae* ATCC BAA-1706 and carbapenem resistant *K. pneumoniae* ATCC BAA-1705 served as the inoculum control. Optical density (OD) of stained adherent bacteria was determined with a micro ELISA (ELX808, Biotek, India) auto reader at a wavelength of 520 nm. These OD values were considered as an index of bacteria adhering to surface and forming biofilms. The experiment was performed in triplicate and the average was derived. To compensate the background absorbance, OD readings from sterile medium, fixative, dye were averaged and subtracted from all the test values. The mean OD value obtained from media control well was deducted from all the test OD values.

Interpretation of bacterial adherence
The bacterial adherence was interpreted based on OD values as

obtained for *A. baumanii* isolate [19]. The mean OD values derived is shown below in **Table 1 (see supplementary material)**

Detection of viability of biofilm producing bacteria after antibacterial treatment:
Production of biofilm
The bacterial isolate was allowed to produce biofilm by inoculating 200μl of 1:10 diluted *A. baumanii* isolate onto three 96 well round bottom tissue culture plate and incubated aerobically at 37⁰C for 24 hours as described earlier [19, 20]. After 24 hr of growth, the biofilm production was checked out in one of the plate by procedure described above.

Antibacterial treatment of Biofilm
After confirming the production of biofilm, the remaining plates were subjected for antimicrobial susceptibility testing by microbroth dilution method. The medium was first removed by aspiration from the wells and subjected for antibiotic treatment with ceftriaxone (Alkem, India), cefepime (Zuventus, India), cefoperazone (Pfizer, India), imepenum (Ranbaxy, India) and meropenum (Blue cross, India). The bacteria were then treated with various concentrations of the antibiotics ranging from 1280mg/L – 10mg/L and incubated for 24 hours at 37°C (carried out in duplicates). After overnight incubation, the medium containing the antimicrobial agent was gently aspirated out.

Assessment of cell morphology by pseudo- confocal microscope
The reduction in the amount of bacterial cell count was observed under Axio Observer fluorescent microscope (Carl Zeiss, Berlin, and Germany). The images were processed using Axio Vision 4.7 software (Carl Zeiss, Bangalore, India).

MTT assay
Following this, the viability of the bacteria in each of the antibiotic concentration was tested by MTT (3-[4, 5-dimethylthiazol-2-yl]-2, 5-diphenyltetrazolium bromide, Invitrogen, India) assay according to the method described by Kairo *et al* (1999) [21]. Briefly, after 24 h lasting antibiotic treatment, the wells of micro plate were aspirated out and filled with 150 μl of PBS per well, then 50μl of MTT solution (0.3% in PBS) was added. Plates were incubated for 2 h at 37°C. At the end of incubation period, MTT was replaced with 150 μl of DMSO (Merck, India). To enable complete dissolving of formed purple formazan crystals, the plates were incubated for 15 minutes at room temperature followed by a gentle agitation for 5 min. The optical density of the wells was calculated through micro ELISA auto reader at wavelength of 550 nm. Cell viability (or cell survival) was calculated as: (Test OD/Control OD) ×100. The 50% inhibitory concentration (IC50) of the five drugs (ceftriaxone, cefepime, cefoperazone, imepenum and meropenum) was computed using polynomial regression analysis using Microsoft Excel.

Conjugation experiment
To obtain the transconjugant, 0.2 ml of an exponentially grown culture of the test strain *A. baumanii* (donor cells) was mixed with 1.8 ml of an overnight culture of *E. coli* XL-1 Blue (recipient cells) in LB broth (Hi media, India). Mixtures were incubated without shaking at 37°C for 18 h. Transconjugants were selected by their ability to resist streptomycin 65 μg/ml (Oxoid),

tetracycline 100 µg/ml (Merck, India) and cefotaxime 2 µg/ml (Himedia, India) incorporated in LB agar **[22, 23]**. The transconjugants were preceded further for the antibiotic susceptibility testing with the same antibiotic which was used for testing parental isolates.

Sequence Retrieval

The Protein sequence for *bla*NDM-1 in *Acinetobacter baumannii* (UniProtKB accession number: F8UNN7) was retrieved from UniProtKB **[24]**. BLASTP search was carried out for this protein against the PDB **[25]** to detect the most suitable template for modeling, wherein, *E. coli bla*NDM-1 crystal structure (PDB id: 3S0Z) was found to have 100% identity. So, the PDB structure 3S0Z was retrieved from the Protein Data Bank and the same was used for structural studies. However, the crystal structure had a missing loop region [167-170] which was modeled and validated by different structural assessment studies **[26]**.

Structure validation

The crystal Structure (3SOZ) was fixed for missing loop, and was examined by using Q-MEAN SERVER, which estimates quality of a model, whereby, it gives two different scores: Global score, which includes Q-Mean Score which is a global score of the whole model reflecting predicted model reliability ranging from 0 to 1, Z-Score which is calculated by relating Q-Mean score to scores of a non-redundant set of high-resolution x-rays structures of similar size. Local Score includes Residue Error which was estimated per residue **[27]**. Ramachandran plot validation was also performed using Structure Analysis & Verification (SAVES) server **[28]**.

Molecular Dynamics (MD) Studies of blaNDM-1 protein

MD Simulation was performed for the modeled protein on OPEN DISCOVERY Linux Platform with pre-installed GROMACS software **[29]** to analyze the stability of the protein. GROMOS96 43a1 **[30]** force field was used. Periodic boundary conditions were applied with 0.9nm of cubic box. The protein was solvated with SPC water model which added 11619 SOL molecules to the system. System was neutralized by replacing water molecules with 10 NA+ counter ions. Steepest Descent algorithm was used for energy minimization which converged in 283 steps. Equilibration of the NVT and NPT ensembles was conducted separately each with 100ps and with 2 fs of integration time steps. The final production run was performed for 5ns. Finally, the decoy with least potential energy was chosen for further studies.

Prediction of Active site

The binding pocket for the target protein was predicted using computed atlas of surface topography of proteins (CASTP) **[31]**. Further, all the binding pockets residues were compared with the documented active site residues the protein **[32]**. Binding Pocket from CASTP was selected which covers all the active site residues of the protein. Finally, this binding pocket was used for further docking studies.

Retrieval of Ligands

The structural coordinates of the ligands were retrieved from Ligand Depot, Pubchem and Drug Bank based on availability. The ligands are Ceftriaxone (Pub Chem: CID 5479530); Cefepime (Pub Chem: CID 5479537); and Cefoperazone (Pub Chem: CID 44185) Carbapenems which includes Imipenum (Drug Bank: DB01598) and Meropenum (PDB ID: 3q82); Optimisation of all the ligands were done in ProDrg server **[33]**.

Molecular Docking Studies

Auto Dock 4.0 **[34]** was used for carrying out docking studies of *bla*NDM-1 protein with all the five different types of ligands. Semi-flexible docking was done in which protein was kept as rigid and the ligands as flexible **[35]**. For all the ligands, the possible torsion angles were set to rotate freely. In the preparation of protein, polar hydrogens were added and kollman united partial charges were also assigned. Gasteiger charges were also assigned to the ligands. Auto Dock 4.0 was compiled and run under Linux operating system. Auto Dock requires pre assigned grid maps, and grid must surround the region of interest in the protein. In this study, binding site residues were generated by CASTp server, which includes all the active site residues were used for setting the grid. The grid box size was set at 100, 100 and 100 Å (x, y and z) and grid center 3.0, 3.0, 3.0 for x, y and z- coordinates for all ligand molecules. The spacing between grid point was 0.375 Å for active site in such a way to surround the entire given binding site residues. The Lamarckian Genetic Algorithm parameter was used for the best docking conformers. The following parameters were followed for all the compounds. A maximum of 10 conformers were considered for each compound, the population size was 150, maximum number of evaluation was set to 2,500,000, maximum number of generations was 27,000, rate of gene mutation was 0.02, rate of crossover was 0.80, GA crossover mode two pt (two point), mean of Cauchy distribution for gene mutation was 0.0, variance of Cauchy distribution for gene mutation was 10.0, and number of generation for picking worst individual was set to 10.
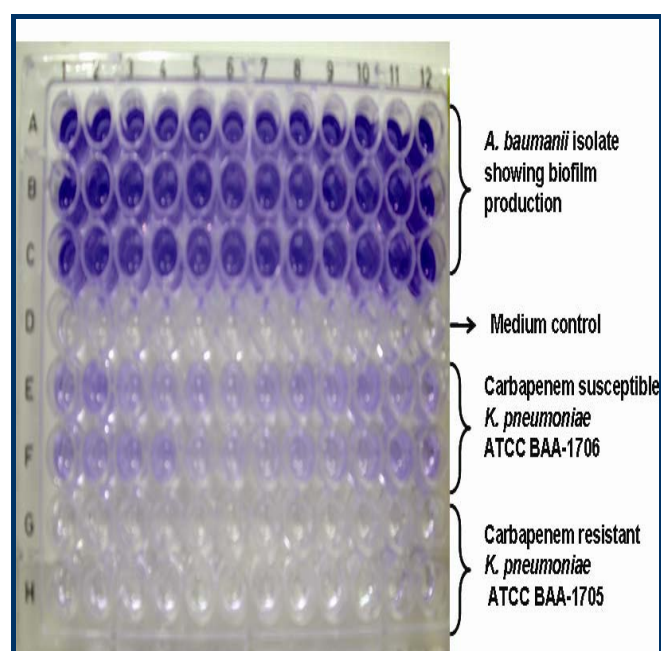

Figure 1: Tissue culture plate showing Biofilm production by *A. baumanii* isolate.

Results:

Results of in vitro biofilm production

The isolate from the donor corneal rim specimen produced high level of biofilm with an OD of 0.361 at an absorbance of 520nm.

BIOINFORMATION

Biofilm produced by the *A. baumannii* isolate is shown in (**Figure 1**).

Results of viability of biofilm producing bacteria after antibacterial treatment

The viability of biofilm producing *A. baumanii* isolate reduced on exposure to antibiotics and was inferred by reduction in the bacterial cell count after antibiotic treatment. (Observed through Axio Observer fluorescent microscope (Carl Zeiss, Berlin, and Germany). The degree of biofilm formation and percent of viability of bacterial cells after antibiotic treatment were analyzed by MTT staining. Higher degree of resistance was observed for all 5 drugs (ceftriaxone, cefepime, cefoperazone, imepenum and meropenum) after 24 hours of antibiotic treatment. The IC_{50} of ceftriaxone, cefepime, cefoperazone, imepenum and meropenum to be 80 mg/L, 80 mg/L, 80 mg/L, 80 mg/L, and 80 mg/L, respectively. Effect of imepenum on *A. baumannii* at various concentrations is shown in (**Figure 2**).
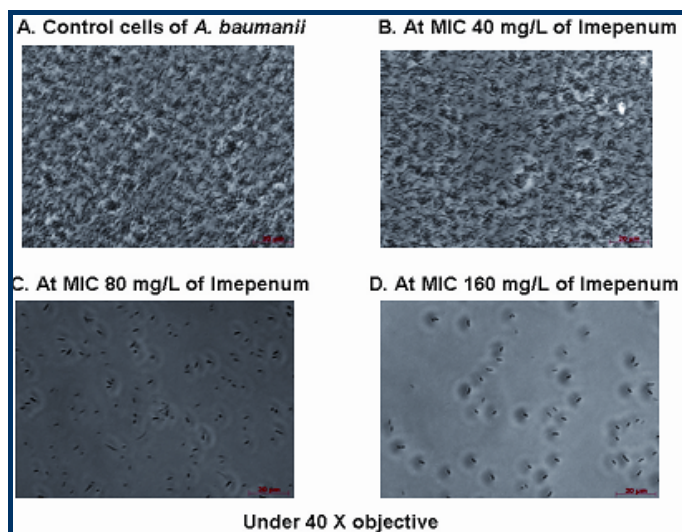

Figure 2: Morphology of *A. baumanii* cells at various concentrations of imepenum are seen under Axio Observer fluorescent microscope (**A**) Control, **B**) At an imepenum concentration of 40 mg/L, **C)** At an imepenum concentration of 80 mg/L and **D)** At an imepenum concentration of 160 mg/L).
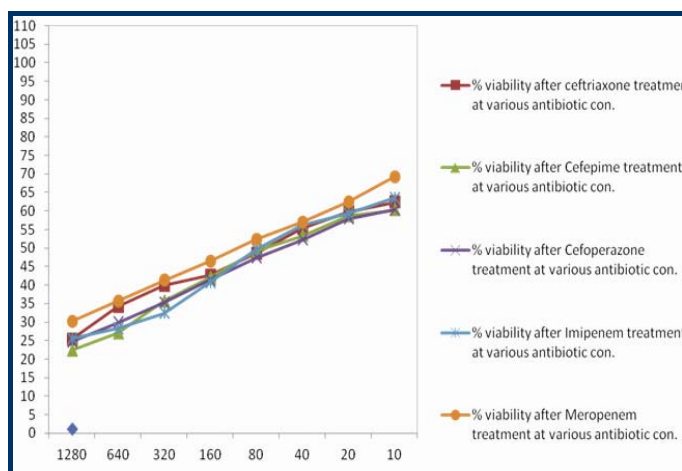

Figure 3: Line graph representing percentage of viability of *A. baumanii* cells to increasing concentrations of antibiotics.

Sensitivity of A. baumanii cells to increasing concentrations of antibiotics

Figure 3 presents the percentage viability of *A. baumannii* at various concentrations of antibiotics ie. ceftriaxone, cefepime, cefoperazone, imepenum and meropenum at increasing dosages higher than their respective IC_{50} at 24 h of treatment. However, at highest dosage, of all five antibiotics at 1280mg/L significant decrease in the cell viability was not observed.

Results of conjugation experiment

Successful transconjugation was noted with the *A. baumannii* isolate that harbored *bla*NDM-1 gene. The transfer of *bla*NDM-1 gene to the *E. coli* XL-1 Blue was confirmed by both PCR and MIC testing. PCR targeting *bla*NDM-1 proved that the transconjugants carried the *bla*NDM-1 gene and MIC results showed similar antibiotic results when compared to the parental donor strains tested. Transconjugants grown in LB medium incorporated with antibiotics is shown in (**Figure 4).**
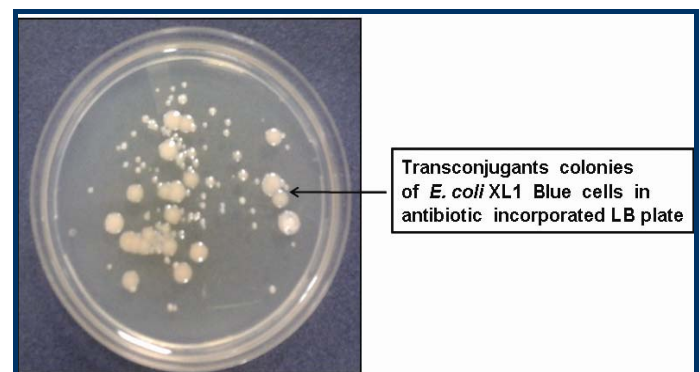

Figure 4: Conjugation experiment showing the growth of transconjugants confirming the ability of transferring genetic material carrying drug resistance genes to competent

Cells *Molecular modelling*

As discussed earlier, the missing residues (167-170) **(Figure 5A)** of 3SOZ_A **[36]** was modeled using Swiss model beta server with advanced modeling option with 3SOZ_A as template. The modeled structure was refined, validated and was utilized for further docking studies.
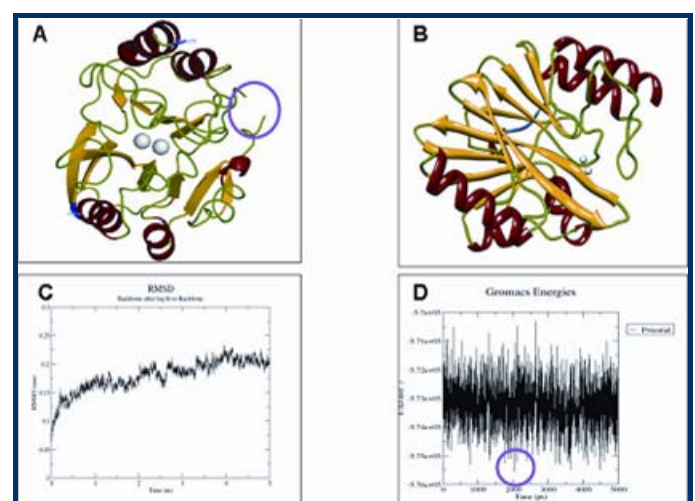

Figure 5: (A) Crystallized 3D structure of blaNDM-1 in *E. coli*. Magenta color circle show missing loop region in this structure;

(B) 3D Structure of blaNDM-1. In this figure red color indicate helix, yellow color indicate beta strand, green color indicate coil, blue color indicate missing loop region of template structure using USCF – CHIMERA; **(C)** C-alpha Backbone residue-wise root mean square deviation (RMSD) of blaNDM-1 at 5ns; **(D)** Potential energy graph over 5ns. The lowest potential energy was noted at 2000ps, marked with a Magenta circle.

Structure validation

The loop fixed model of *bla*NDM-1 was subjected to further structural validation through Q-mean server. This server predicted a structure score of 0.68. The PROCHECK analysis shows 92.1% residues in favored regions, 7.9% in allowed region and 0% in disallowed region. The final refined structure of *bla*NDM-1 was used for further molecular dynamics simulation studies **(Figure 5B)**.

Molecular dynamics studies

Molecular Dynamics simulation for 5 nanoseconds revealed the conformational changes and stability of the protein in response to optimal ensemble conditions as shown in (**Figure 5c**). The Potential energy traces a reliable drop in value over 5ns of MD simulation, with the lowest potential energy structure observed at 2000ps as shown in **(Figure 5d)**.
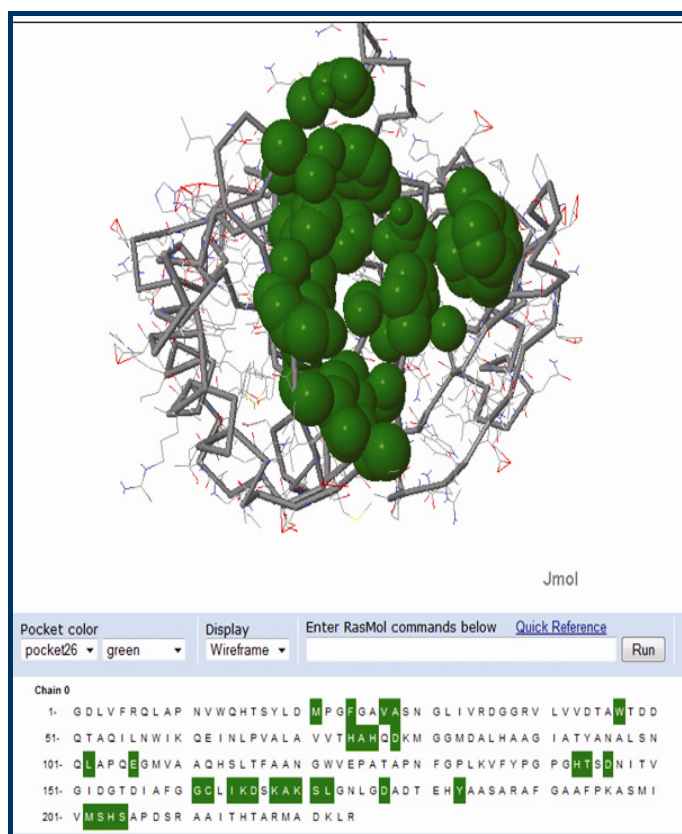

Figure 6: Active site pocket of blaNDM-1. Wire frame illustrated in overall protein and Green color ball illustrated in active site residues.

Active site prediction

Active site pocket idenitification was performed using CASTP Server, which predicted 26 different pockets with varied Area and Volume. Each pocket conformation presents residues that matched with the structure of *bla*NDM-1 in *E. coli* [PDB id:

3SOZ_A] **[32]**. Overall documented active site residues of *bla*NDM-1 were corresponding to the 26th pocket (Met21, Phe24, Val27, Ala28, Trp47, His74, His76, Asp78, Leu102, Glu106, His143, Thr146, Gly161, Cys162, Ile164, Lys165, Asp166, Lys168, Ala169, Lys170, Ser171, Leu172, Asp177, Tyr183, Met202, Ser203, His 204, and Ser205) as shown in **(Figure 6).**

Ligand optimization

All the ligands were retrieved from Ligand Depot, Pubchem and Drug Bank based on availability. These ligands were minimization using for using GROMOS forcefield option of PRODRG Server and was further used of docking studies.

Docking studies of blaNDM-1

Docking studies of the chosen ligands were performed on the predicted active site region of *bla*NDM-1. The binding energy of all the interactions reveal that, among all the ligands, the highest binding affinity of (-6.17Kcal/mol) was observed for Cefoperazone. The detailed hydrogen bonding interactions and inhibitory constant value of *bla*NDM-1 with all the ligands are shown in (**Figure 7**), and **Table 2 (see supplementary material)** respectively. The docking studies show hydrophobic interactions, and hydrogen bonds, which very well correlated with the documented studies.
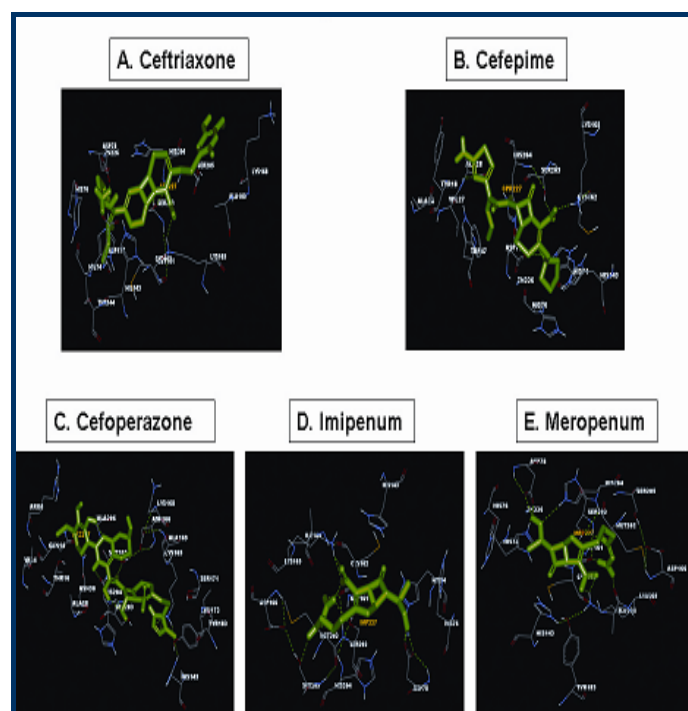

Figure 7: Docking studies of blaNDM-1 protein with all the inhibitors. Green color sticks indicates ligand, Green color doted lines hydrogen bond.

Ceftriaxone

Lys 165, Ser 203 and Asp 177 were found to form 3 hydrogen bonds with that of ceftriaxone **(Figure 7A)**. These hydrogen bonds were found to stabilize the binding of ceftriaxone. The IC_{50} of the drug was found to be 144.25μM.

Cefepime

The result of cefepime docking into the reported active site of *bla*NDM-1 is shown in **(Figure 7B)**. Under careful observation

three hydrogen bonds were found to be formed with the following residues: Lys 165, Ser 203 and Ala 28. The IC$_{50}$ of the drug was found to be 166.4µM.

Cefoperazone

Cefoperazone was found to dock into the reported active site of *bla*NDM-1 is shown in **(Figure 7C)**. A through examination of the binding pocket indicated that cefoperazone formed three hydrogen bonds with the residue of Ser 205, Lys 165 and His 204. The IC$_{50}$ of the drug was found to be 123.90µM.

Imepenum

Lys 165, Ser 203, Gly 161, Asp 78 and Ser 205 were found to form 5 hydrogen bonds with that of Imepenum is shown in **(Figure 7D)**. These hydrogen bonds were found to stabilize the binding of imepenum. The IC$_{50}$ of the drug was found to be 267.24µM.

Meropenum

The result of meropenum docking into the reported active site of *bla*NDM-1 is shown in **(Figure 7E)**. Under careful observation six hydrogen bonds were found to be formed with the following residues: Lys 165, Ser 203, Gly 161, Asp 78, Ile 164 and His 204. The IC$_{50}$ of the drug was found to be 208.62µM.

Discussion:

Over the past decade, increased prevalence of multidrug-resistant strains of *A. baumannii* (MDR-AB) has been reported. The prevalence of strains resistant to the usually potent and safe β-lactam antibiotics, such as ampicillin-sulbactam and carbapenems, had increased substantially **[36-40]**. Since the new antimicrobial agents for Gram-negative pathogens shrinks, the longevity of existing compounds becomes a matter of primary concern **[41]**. Many *Acinetobacter* are now resistant to commonly used antibacterial drugs, including penicillins, expanded-spectrum cephalosporins **[38, 42]** cephamycins, aminoglycosides **[43]** chloramphenicol, and tetracyclines **[37]**. Carbapenems have become the drugs of choice against *Acinetobacter* infections in many centers but are slowly being compromised by the emergence of carbapenem-hydrolyzing ß-lactamases **[44]**. Most potent emerging carbapenemase gene is New Delhi metallo-beta-lactamases (*bla*NDM-1). The first clue for the presence of a carbapenemase was inferred from the increased minimum inhibitory concentration (MIC) especially to imipenem, or meropenem. In our previous study, MIC results of *A. baumannii* isolate showed resistance to Ceftazidime, Ceftriaxone, Cefoperazone/Sulbactum, Cefepime, Imipenum and Meropenum (Data not shown for reference). In the current study, the MIC data and the docking results were in concordance and resistance could be attributed to the biofilm production. The reproducibility of obtained experimental results confirmed the predictive accuracy. Yong *et al.*, 2009 documented cephalosporins group of antibiotics as most potential inhibitors of *bla*NDM1, which was observed in our study in terms of Biofilm production and inhibitory mode of interactions. However, carbapenem group of antibiotics studied were proven to be more significant when compared to cephalosporins. Liang Z, (2011) *et al.* **[45]** has reported *bla*NDM-1 contains an additional insert between residues 162 and 166, which is not present in other MBLs. Since the insert is in the opposite side of the active site, with a distance of around 20 Å, its role in the hydrolysis reaction is still unknown. Interestingly, in our study we found both cephalosporins to interact with LYS

165, whist, carbapenem group was found to interact with GLY161 and LYS165. However, this prediction needs to be confirmed by other structural biology methods.

Conclusion:

We have demonstrated the correlation between *bla*NDM–1 positivity, and biofilm production with molecular interactions inferred through *in silico* docking studies which have attributed to high level resistance. Further by this study, we also highlight the importance of 162-166 region of *bla*NDM-1 as a potential site for drug targeting.

References:

[1] Féria C *et al*. *J Antimicrob Chemother.* 2002 **49**: 7 PMID: 11751770]

[2] Yong *D et al. Antimicrob Agents Chemother.* 2009 **53**: 12 [PMID: 2786356]

[3] Paterson DL *et al. Am J Med.* 2006 **119**: S20 [PMID: 16735147]

[4] Sekizuka T *et al. T plos one.* 2011 **6**: 9

[5] Kim Y *et al. T plos one.* 2011 **6**: 9

[6] Wang JF *et al.* T *plos one.* 2011 **6**: 4.

[7] Struelens MJ *et al. Euro Surveill.* 2010 **15**: 19716 [PMID: 21144431]

[8] Rolain JM *et al. Clin Microbiol Infec* 2010 **16**: 1699 [PMID: 20874758]

[9] Diene SM *et al. Int J Antimicrob Agents* 2011 **37**: 6 [PMID: 21497063]

[10] Poirel L *et al. Antimicrob Agents Chemother.* 2010 **54**: 4914 [PMID: 20823289]

[11] KK Kumarasamy *et al. Lancet Infect Dis.* 2010 **10**: 597 [PMID: 20705517]

[12] Chen Y *et al.* J *Antimicrob Chemother.* 2011 **66**: 1255 [PMID: 21398294]

[13] Nemec A *et al.* *J Antimicrob Chemother.* 2008 **62**: 484 [PMID: 18477708]

[14] Poirel L *et al.* *J Antimicrob Chemother.* 2011 **66**: 2781 [PMID: 21930570]

[15] Maragakis LL & Perl TM, *Clin Infect Dis* 2008 **46**: 1254 [PMID: 18444865]

[16] Murali S *et al. Curr Eye Res.* 2012 **37**: 195 [PMID:22335806]

[17] Kaase M *et al. J Antimicrob Chemother.* 2011 **66**: 1260 [PMID: 21427107]

[18] Folkens AT *et al. Infection of the eye.* 1996 **5**: 93.

[19] Mathur T *et al. Indian J Med Microbiol.* 2006 **24**: 25 [PMID:16505551]

[20] Coenye T *et al. Res Microbiol.* 2007 **158**: 386 [PMID:17399956]

[21] Kairo SK *et al. Vaccines.* 1999 **17**: 2423 [PMID: 10392624]

[22] Cartelle M *et al. Antimicrob Agents Chemother.* 2004 **48**: 2308 [PMID: 15155242]

[23] Is Hamad *et al. J Duhok Univ.* 2008 **12**: 1

[24] http://www.uniprot.org/

[25] http://www.rscb.org/pdb/

[26] Kiefer F *et al. Nucleic Acids Res.* 2009 **37: D387** [PMID: 18931379]

[27] Benkert P *et al. Nucleic Acids Res.* 2009 **37: W510** [PMCID: PMC2703985]

BIOINFORMATION

[28] http://www.ebi.ac.uk/thornton srv/software/PROCHECK/refs.html .

[29] Vetrivel U & Pilla K, *Bioinformation*. 2008 **3**: 144 [PMID: 19238235]

[30] Hess B *et al. J Chem Theory Comput.* 2008 **4**: 3 doi:10.1021/ct700301q

[31] Liang JJ *et al. Protein Sci.* 1998 **7**: 1884 [PMID: 9761470]

[32] Guo Y *et al. Protein Cell*. 2011 **2**: 384 [PMID: 21637961]

[33] Schüttelkopf AW *et al. Acta Crystalloqr D Biol Crystallogr.* 2004 **60**: 1355 [PMID: 15272157]

[34] Huey R *et al. J Comput Chem.* 2007 **30**: 1145 [PMID: 17274016]

[35] Deepa et al. *J ocul bio dis infor.* 2010 **3**: DOI: 10.1007/s12177-011-9065-7

[36] Young LS *et al. Infect Control Hosp Epidemiol*. 2007 **28**: 1247 [PMID:17926275]

[37] Bergogne-Berezin E & Towner KJ, *Clin Microbiol Rev.* 1996 **9**: 148 **[**PMID:8964033]

[38] Reddy T *et al. Antimicrob Agents Chemother.* 2010 **54**: 2235 [PMID: 20211887]

[39] Bassetti M *et al. Future Microbiol*. 2008 **3**: 649 [PMID:19072182]

[40] Falagas *et al. Eur J Clin Microbiol Infect Dis.* 2007 **26**:12 [PMID: 17701432]

[41] Eagye KJ *et al. Ann Clin Microbiol Antimicrob.* 2007 **6**: 11 [PMID: 17908321]

[42] Morohoshi T *et al. J Antibiot.* 1977 **30**: 969

[43] Dowding JE *et al. J Gen Microbiol.* 1976 **110**: 239 [PMID: 430029]

[44] Dalla-Costa LM *et al. J Clin Microbiol.* 2003 **41**: 3403 [PMID: 12843104]

[45] Liang Z *PLoS ONE*. 2011 **6**: 8

Supplementary material:

Table 1: Classification of bacterial adherence by Tissue Culture Plate method

Mean OD values	Adherence	Biofilm formation
<0.120	Non	Non / weak
0.120-0.240	Moderate	Moderat
>0.240	Strong	High

Table 2: Showing the docking results of docking interactions and IC50 calculation.

Ligands	Binding Energy (Kcal/mol)	No. of H-bonds	H- BONDS	Ic $_{50}$ of BiofilmMTT Assay (mg/L)	Experimental IC$_{50}$ (µM)
Ceftriaxone	-5.68	3	LYS 165, SER 203, ASP 177	80	144.25
Cefepime	-5.48	3	LYS 165, SER 203, ALA 28	80	166.47
Cefoperazone	-6.17	3	SER 205, LYS 165, HIS 204	80	123.90
Imipenem	-5.61	5	LYS 165, SER 203, GLY 161, ASP 78, SER 205	80	267.24
Meropenem	-4.74	6	LYS 165, SER 203, GLY 161, ASP 78, ILE 164, HIS 204	80	208.62